

# RSC Advances



This is an *Accepted Manuscript*, which has been through the Royal Society of Chemistry peer review process and has been accepted for publication.

*Accepted Manuscripts* are published online shortly after acceptance, before technical editing, formatting and proof reading. Using this free service, authors can make their results available to the community, in citable form, before we publish the edited article. This *Accepted Manuscript* will be replaced by the edited, formatted and paginated article as soon as this is available.

You can find more information about *Accepted Manuscripts* in the [Information for Authors](#).

Please note that technical editing may introduce minor changes to the text and/or graphics, which may alter content. The journal's standard [Terms & Conditions](#) and the [Ethical guidelines](#) still apply. In no event shall the Royal Society of Chemistry be held responsible for any errors or omissions in this *Accepted Manuscript* or any consequences arising from the use of any information it contains.

## ARTICLE

## Formation and Phase Transition of Hydrogel in Zwitterionic/Anionic Surfactant System

Cite this: DOI:

10.1039/x0xx00000x

Haiming Fan,<sup>\*a,b</sup> Shuzhi Zhao,<sup>a</sup> Bingcheng Li,<sup>a</sup> Haijian Fan,<sup>a</sup> Wanli Kang<sup>a</sup> and Jianbin Huang,<sup>\*a,c</sup>Received 00th January 2015,  
Accepted 00th January 2015

DOI: 10.1039/x0xx00000x

[www.rsc.org/](http://www.rsc.org/)

The phase behavior and microstructure in a mixture of zwitterionic surfactant N-hexadecyl-N,N-dimethyl-3-ammonio-1-propane sulfonate (HDPS) and anionic surfactant sodium dodecylsulfate (SDS) were studied. Macroscopic appearance, tube inversion test and rheological measurement are employed to characterize the phase behavior and it was found hydrogel formed in an appropriate total concentration ( $C_T$ ) and molar percentage of SDS ( $X_{SDS}$ ) at 25 °C for HDPS/SDS systems. Microstructures in the hydrogel were identified to be long wormlike micelle and small spherical vesicles by transmission electron microscopy (TEM). The coexistence of wormlike micelles and small vesicles brings an appropriate packing parameter ( $p$ ), which makes the wormlike micelles reach enough length and entangled to three-dimensional elastic hydrogel. The HDPS/SDS hydrogel transforms into viscoelastic sol upon increasing temperature and the determined gel-sol transition temperature ( $T_{g-s}$ ) is around 30 °C by optical and rheological method. Besides, adding salt makes the wormlike micelle lengthened and the solution rheological properties reinforced. Even it may induce a sol-gel phase transition for mixed zwitterionic and anionic surfactant systems.

### Introduction

Hydrogels have attracted considerable growing interest because of their unique features and potential applications such as sensors or optical components,<sup>1,2</sup> scaffolds for tissue engineering<sup>3,4</sup>, template for nanomaterial synthesis<sup>5-8</sup> and carriers for drug release and delivery<sup>9,10</sup>. The formation of hydrogels has been well documented with biopolymers such as collagen, hyaluronic acid, fibrin, alginate, F-actin and chitosan, and also synthetic polymers generated from derivatives of poly(hydroxyethyl methacrylate) (HEMA), poly(ethylene glycol) (PEG), poly(vinyl alcohol), poly(acrylic acid), poly(methacrylic acid), polyacrylamide and other derivatives.<sup>11, 12</sup> Gelation with polymeric gelators is believed to occur by chemical and/or physical cross-linking of polymeric chains, leading to the formation of a highly intertwined three-dimensional network, which restrains water molecules by surface tension. On the other hand, low-molecular-mass hydrogelators create three-dimensional network structures through molecular self-assembles driven by noncovalent physical interactions and gelation results from a balance of solubilization and crystallization.<sup>13-15</sup> A wide variety of molecular species have been discovered to act as hydrogelators during the last few decades including amino acid derivatives, polypeptides, carbohydrate derivatives, bile acid, lipids and

surfactants. Compared to polymeric hydrogelators, these small molecule hydrogelators offer the advantage of easily controllable gel properties by changing parameters such as the temperature, pH value, salinity or mechanical agitation. Furthermore, they are easier to degrade than most polymers which benefit biological application.

Surfactants are one particularly interesting class of hydrogelators.<sup>15-18</sup> Surfactant molecules are often well soluble in water as well as they self-assemble into various aggregates such as wormlike micelle,<sup>19-23</sup> vesicle,<sup>24-26</sup> lamellar,<sup>27-29</sup> nanofiber and microtube<sup>30-36</sup> in aqueous solution above the so-called critical micelle concentration. These aggregates have shown the ability to build stable hydrogels. For example, Gradziński et al.<sup>25</sup> studied the gel phase formed in tetradecyldimethylamine oxide (TDMAO)/ tetradecyltrimethylammonium bromide (TTABr) mixed systems, and the formation of hydrogel was attributed to densely packed monodisperse and unilamellar vesicles. González et al.<sup>34</sup> investigated the effect of pH on the phase behavior of sodium dodecylsulfate (SDS)/lystine mixtures, and it was found hundreds of micrometers long fibers entangled to form gels. Lin et al.<sup>35</sup> found that elastic hydrogel formed in a mixture of 1-hexadecyl-3-methylimidazolium bromide (C16MIMBr) and sodium salicylate (NaSal) and attributed it to the crystallization of wormlike micelles. And more important, to achieve the

required balance of solubilization and crystallization for hydrogel formation, the interaction between the aggregates can be modulated and optimized by careful adjusting environmental factors (e.g., concentration, composition, temperature, pH, salt et al) and the surfactant molecular structures (e.g., the nature of the headgroup, the length and architecture of the hydrophobic tail, the spacer length for Gemini and Bola surfactants).

Zwitterionic surfactants are interesting molecules owing to their low toxicity, high foam stability and resistance to hard water.<sup>19, 20, 36-47</sup> In previous works, Kumar et al.<sup>19</sup> found that elastic hydrogel formed by zwitterionic surfactant erucyl dimethyl amidopropyl betaine(EDAB, C<sub>22</sub>-unsaturated tailed) and Chu et al.<sup>20</sup> also found hydrogel formed by concentrated 3-(N-erucamido-propyl-N,N-dimethyl ammonium) propane-sulfonate (EDAS, C<sub>22</sub>-unsaturated tailed) in the presence of NaCl. The long-chain zwitterionic surfactants are hard to be soluble in water, and the unsaturated carbon-carbon double bond and amido group in the hydrophobic tail of EDAB and EDAS can enhance the solubility, but also make the surfactant easily to lose gelation activity by oxidation and hydrolysis.<sup>36</sup> For short-chain zwitterionic surfactants, it has been reported by Lopez-Diaz et al., Qiao et al. and Fan et al. that viscoelastic solution with wormlike micelles formed in the aqueous mixtures of N-dodecyl-N,N-dimethyl-3-ammonio-1-propane sulfonate (DDPS, C<sub>12</sub>-saturated tailed) or tetradecyl dimethyl-ammonium propane sulfonate(TDPS, C<sub>14</sub>-saturated tailed) and SDS.<sup>39-41</sup> Compared these reported phase behavior and microstructure results of short-chain and long-chain zwitterionic surfactant solutions, the microstructures are all wormlike micelles, but the wormlike micelles formed by long-chain zwitterionic surfactants are longer, which led to a surprising result that the solutions behave like an elastic gel with an infinite relaxation time and can support their own weight. Herein, the phase behavior is studied in the mixed system of zwitterionic surfactant N-hexadecyl-N,N-dimethyl-3-ammonio-1-propane sulfonate (HDPS, C<sub>16</sub>-saturated tailed) and anionic surfactant sodium dodecylsulfate (SDS). This selection involves two important considerations, namely (i) using a medium length saturated chain zwitterionic surfactant (HDPS) to avoid insoluble and instability; (ii) adding anionic surfactant to promote the formation of long wormlike micelle. It is found that hydrogel formed in HDPS/SDS systems by changing the total concentration ( $C_T$ ) and molar percentage of SDS ( $X_{SDS}$ ). Microstructures in the hydrogel are coexistence of long wormlike micelles and small vesicles, which is why hydrogel can be found in HDPS/SDS surfactant systems but not in TDPS/SDS and DDPS/SDS surfactant systems. Moreover, the effects of temperature and salt on the sol-gel phase transition are investigated to understand the general rules for hydrogel formation in mixed zwitterionic/anionic surfactant systems.

## Experimental

### Materials

N-hexadecyl-N,N-dimethyl-3-ammonio-1-propane sulfonate (HDPS, J&K Chemical,  $\geq 99\%$ ), N-tetradecyl-N,N-dimethyl-3-ammonio-1-

propane sulfonate (TDPS, J&K Chemical,  $\geq 99\%$ ), N-dodecyl-N,N-dimethyl-3-ammonio-1-propane sulfonate (DDPS, Fluka,  $\geq 97\%$ ), sodium dodecylsulfate(SDS, Alfa Aesar,  $>99\%$ ), NaCl (Beijing Chemical Co.,A.R. grade) were used as received. The water used was bidistilled from potassium permanganate containing deionized water to remove traces of organic compounds.

### Sample Preparation

Samples were prepared by mixing the individual surfactant aqueous solution directly in a test tube at certain total concentrations and molar percentages of SDS. The molar percentages of SDS,  $X_{SDS}$ , is defined as  $X_{SDS}=[SDS]/C_T$ , where  $C_T$  (mmol·L<sup>-1</sup>) is the total concentration of surfactants in the system. Then the desired amount of inorganic salt was added to the tube. After sealing, these samples were vortex-mixed and equilibrated at high temperature ( $\sim 70^\circ\text{C}$ ) for 1 h to ensure complete solubility and uniformity. The resulting mixture was maintained in a  $25^\circ\text{C}$  thermostatic bath at least for 72 h before measurements. All measurements are performed at  $25^\circ\text{C}$  without specific documented.

### Rheology Measurements

The rheological properties of samples are measured with a conventional rheometer (Physica MCR301, Anton Paar, Graz). A cone-plate sensor is used with a plate diameter of 49.959mm, a cone angle of  $1^\circ$  and a default gap of 0.047mm. A chamber that covers the sample is used to avoid evaporation. Frequency sweep measurements are carried out from 0.05 to 100 rad.s<sup>-1</sup> in the linear viscoelastic region determined via dynamic strain sweep measurements.

### Transmission Electron Microscopy (TEM)

Micrographs were obtained with a JEM-100CX II transmission electron microscope by negative-staining method using uranyl acetate.

### Transmittance Measurement

The transmittance measurements are obtained by using a Turbiscan MA2000 (Formulation, France) with a pulsed near-infrared light source ( $\lambda=880\text{nm}$ ) to measure the average transmittance.<sup>48</sup> The gel in a test tube is placed in the instrument and the light transmitted from the sample is then measured periodically along the height at different temperature. The results are presented as the transmittance changes as a function of sample height.

## Results and discussion

### Phase Behavior and Hydrogel Formation

The phase behavior of aqueous mixtures of HDPS and SDS at 100 mmol·L<sup>-1</sup> total concentration ( $C_T$ ) was investigated for six different molar percentages of SDS ( $X_{SDS}$ ) as shown in Fig.1. It has been found that samples at  $X_{SDS}=0.1$  and  $X_{SDS}=0.2$  are transparent viscoelastic isotropic solutions, which are the typical features of samples containing wormlike micelles and similar with the previous reported results in TDPS/SDS surfactant systems.<sup>39-41</sup> At  $X_{SDS}=0.6$ , the sample is opalescent viscoelastic solution with birefringence viewed under crossed polarizer characterizing the existence of

lamellar phase.<sup>49-51</sup> These samples all flow to the bottom in the tube inversion test. However, in the region with  $X_{\text{SDS}}$  ranging from 0.3 to 0.5, the samples are opalescent hydrogel that can support their own weight in inverted tubes. It is worth noting that we also studied the phase behavior of TDPS/SDS and DDPS/SDS surfactant systems at the same conditions or more concentrated solutions, and hydrogel can be only observed in HDPS/SDS surfactant system.



**Fig. 1** Macroscopic appearance (a) and the tube inversion test (b) of HDPS/SDS mixed surfactant solutions ( $C_T=100 \text{ mmol}\cdot\text{L}^{-1}$ ). The numbers in the photos are the molar percentages of SDS ( $X_{\text{SDS}}$ ).

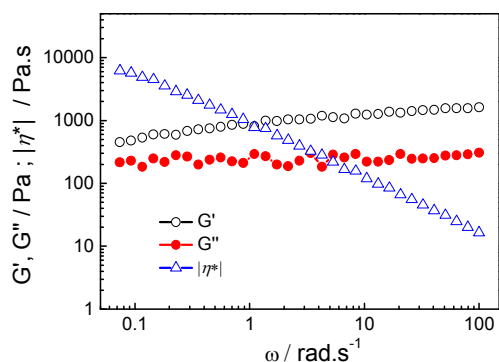


**Fig. 2** Frequency dependence of the elastic modulus ( $G'$ ), viscous modulus ( $G''$ ) and the complex viscosity ( $|\eta^*|$ ) of HDPS/SDS hydrogel ( $C_T=100 \text{ mmol}\cdot\text{L}^{-1}$ ,  $X_{\text{SDS}}=0.4$ ).

The formation of hydrogel is further proved by dynamic rheological measurement and the HDPS/SDS mixture at  $X_{\text{SDS}}=0.4$  was chose as illustration (Fig.2). It shows viscoelastic behavior in which the elastic modulus ( $G'$ ) and the viscous modulus ( $G''$ ) slightly change with the increase of frequency ( $\omega$ ) and the complex viscosity ( $|\eta^*|$ ) varies as  $|\eta^*|\sim\omega^{-1}$ , while the values of  $G'$  ( $\sim 800 \text{ Pa}$ ) is always larger than that of  $G''$  ( $\sim 200 \text{ Pa}$ ) in the entire investigated frequency range. From a rheological standpoint, these above results indicate an elastic gel rheological behavior with infinite relaxation time for the sample.<sup>52</sup> A study is also made of the effect of molar percentage  $X_{\text{SDS}}$  and total concentration on the  $G'$  and  $G''$  of HDPS/SDS mixed surfactant solutions. As is shown in Fig.3a, the  $G'$  exceeding  $G''$  and both values over 100 Pa are observed for  $X_{\text{SDS}}=0.3\sim 0.5$  at  $100 \text{ mmol}\cdot\text{L}^{-1}$  total concentration, which demonstrates the hydrogel

formed and is in agreement with the macroscopic appearance results. Fig.3b shows the values of  $G'$  and  $G''$  as a function of the total concentration, and it has been found the hydrogel can be obtained at the concentration larger than  $30 \text{ mmol}\cdot\text{L}^{-1}$  for  $X_{\text{SDS}}=0.4$ .

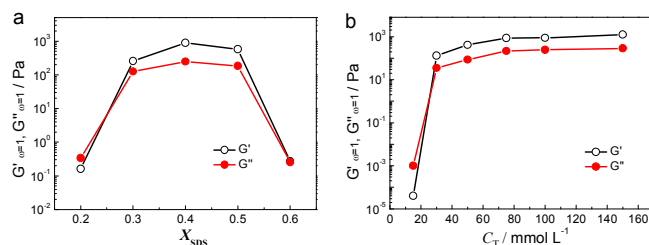


**Fig. 3** Variation of elastic modulus ( $G'$ , open symbols) and viscous modulus ( $G''$ , filled symbols) of HDPS/SDS mixed surfactant solutions with the mixed molar percentage (a,  $C_T=100 \text{ mmol}\cdot\text{L}^{-1}$ ) and total concentration (b,  $X_{\text{SDS}}=0.4$ ) at a fixed angular frequency ( $\omega=1 \text{ rad}\cdot\text{s}^{-1}$ ).

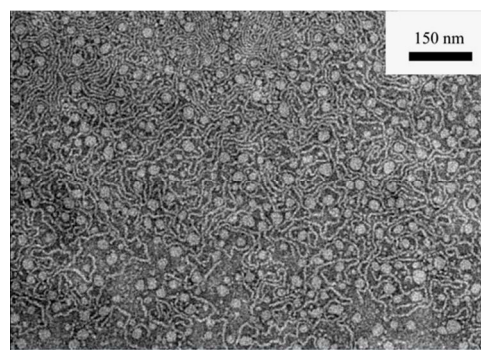


**Fig. 4** TEM image of the HDPS/SDS hydrogel ( $C_T=100 \text{ mmol}\cdot\text{L}^{-1}$ ,  $X_{\text{SDS}}=0.4$ ).

Transmission electron microscopy (TEM) was employed to study the microstructure in HDPS/SDS hydrogel. As is shown in Fig.4, a large number of long wormlike micelles and small spherical vesicles are observed, which gives a deeper understanding for the above phase behavior results. Firstly, the mechanisms of aggregate microstructures formation and transformation can be realized by the well-known theory of packing parameter  $p$ , proposed by Israelachvili et al.,<sup>53, 54</sup> which has been widely and successfully used to explain the aggregate microstructures in surfactant solutions:  $1/3 \leq p < 1/2$  for cylindrical micelles,  $1/2 \leq p < 1$  for bilayer structures and  $p=1$  for planar extended bilayers. The synergistic interaction between zwitterionic and anionic surfactants reduces the repulsion force between surfactant headgroups and then increases the aggregate packing parameter  $p$ . Hence, the wormlike micelles in HDPS/SDS surfactant system grow in contour length and the aggregate microstructures undergo transitions from wormlike micelle to wormlike micelle/vesicle coexistence and then to lamellar structure upon increasing  $X_{\text{SDS}}$  as observed in Fig.1. Secondly, the coexistence of wormlike micelles and small vesicles brings an appropriate packing parameter  $p$ , which makes the wormlike micelles reach enough length and entangled to three-dimensional elastic hydrogel. Thirdly, the packing parameter  $p$  also increases with increasing the hydrophobic tail length of zwitterionic surfactants. Thus, the

wormlike micelles formed in HDPS/SDS mixtures are longer than those in TDPS/SDS and DDPS/SDS mixtures at the same condition. That is why hydrogel can be found in HDPS/SDS surfactant systems but not in TDPS/SDS and DDPS/SDS surfactant systems.

### Thermo-reversible Sol-gel Phase Transition

The hydrogel formed in HDPS/SDS system undergoes gel-sol transition similar to other surfactant-based hydrogel and the microstructure transitioned from entangled long wormlike micelles to short rodlike micelles upon increasing temperature.<sup>17, 18</sup> This phase transition process is first studied by an optical analyzer, Turbiscan MA2000. The hydrogel was equilibrated at different temperature for 2h and the transmittance changes are detected as a function of sample height for the HDPS/SDS hydrogel at  $C_T=100 \text{ mmol}\cdot\text{L}^{-1}$  and  $X_{\text{SDS}}=0.3$ . It can be seen from Fig.5a, at temperature below 28 °C, the sample is opalescent hydrogel and the transmittance approaches to zero. As the temperature increases to 29 °C, the sample becomes clearer and more light is transmitted, whereas it exhibits the hydrogel characteristics by supporting its own weight in inverted tubes. When the temperature is higher than 30 °C, the solution is transparent fluid and about 90% incident light is transmitted. It can be inferred that the system is in a sol state in this regime. The transmittances at 20 mm sample height are presented as a function of temperature in a stepwise heating-cooling cycle (Fig.5b). It is clearly seen that the transmittance at each temperature can be repeated simply by heating or cooling, which indicates that sol-gel phase transition is thermo-reversible. Herein, the gel-sol transition temperature ( $T_{\text{g-s}}$ ) is 30 °C for the HDPS/SDS hydrogel at  $C_T=100 \text{ mmol}\cdot\text{L}^{-1}$  and  $X_{\text{SDS}}=0.3$  from the viewpoint of optical method.

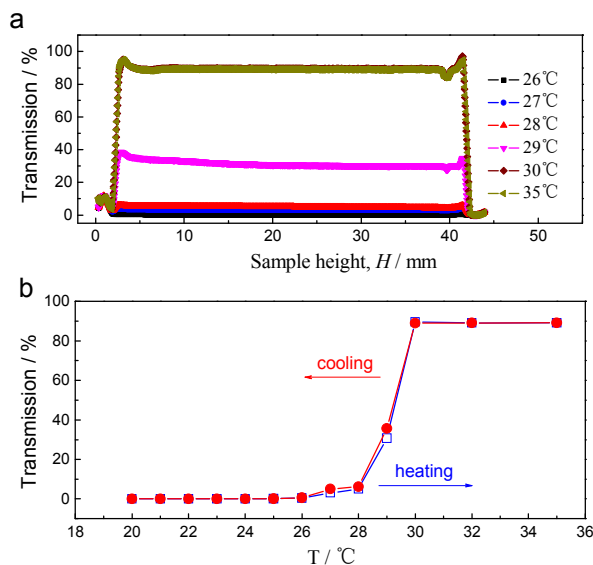


**Fig. 5** The transmittance for the HDPS/SDS hydrogel ( $C_T=100 \text{ mmol}\cdot\text{L}^{-1}$ ,  $X_{\text{SDS}}=0.3$ ) at different sample height (a) and temperature (b).

The gel-sol phase transition of the above sample was further studied with oscillatory rheological experiment. The elastic module  $G'$  were continuous measured at  $6.28 \text{ rad}\cdot\text{s}^{-1}$  while heating at each temperature for 400 s and then increasing to next temperature with

the speed of  $0.01 \text{ }^\circ\text{C}\cdot\text{s}^{-1}$ . This procedure aims to give the sample enough time to fully equilibrate at every temperature and reduce the water evaporation by shortening the measurement time. Then, the measured  $G'$  was normalized as plotted in Fig.6. For the HDPS/SDS hydrogel at  $C_T=100 \text{ mmol}\cdot\text{L}^{-1}$  and  $X_{\text{SDS}}=0.3$ , the normalized elastic modulus ( $G'_N$ ) slightly decreases but still larger than 0.5 below 29 °C, which infers that the gel structure is kept. At 30 °C,  $G'_N$  drops dramatically over three-order of magnitude, suggesting that the gel is transition to sol. All these results are in good agreement with the gel-sol transition monitoring by optical method. As reported by many researchers, the gel-sol transition temperature ( $T_{\text{g-s}}$ ) can be determined from the sharp decrease of the  $G'_N$  curve in rheological measurement.<sup>55, 56</sup> The obtained  $T_{\text{g-s}}$  of  $X_{\text{SDS}}=0.3, 0.4$  and  $0.5$  are 30 °C, 31 °C and 29 °C for  $100 \text{ mmol}\cdot\text{L}^{-1}$  HDPS/SDS hydrogel, respectively.

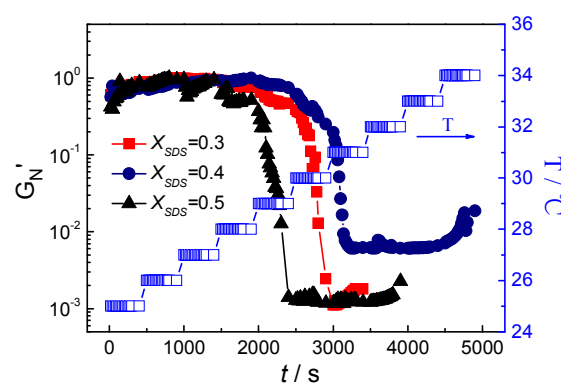


**Fig. 6** Variation of normalized elastic modulus ( $G'_N$ ) at  $6.28 \text{ rad}\cdot\text{s}^{-1}$  with time for the hydrogel ( $C_T=100 \text{ mmol}\cdot\text{L}^{-1}$ ) while heating at each temperature for 400 s and then increasing to next temperature with the speed of  $0.01 \text{ }^\circ\text{C}\cdot\text{s}^{-1}$ .

### Salt-induced Sol-gel Phase Transition

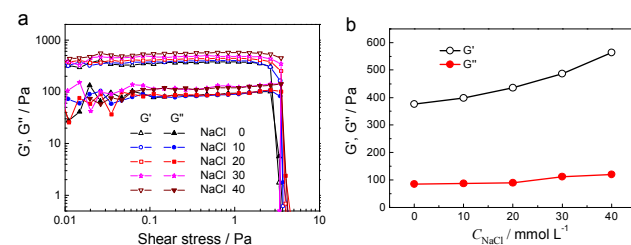


**Fig. 7** (a) Dynamic stress sweep of the HDPS/SDS hydrogel ( $C_T=50 \text{ mmol}\cdot\text{L}^{-1}$ ,  $X_{\text{SDS}}=0.4$ ) at a fixed angular frequency ( $\omega=1 \text{ rad}\cdot\text{s}^{-1}$ ); (b) Elastic modulus ( $G'$ ) and viscous modulus ( $G''$ ) as functions of NaCl concentration.

Hydrogel formed in HDPS/SDS surfactant system is owing to the existence of wormlike micelle with enough contour length. Therefore, the controlling factors for wormlike micelle growth are expected to affect the HDPS/SDS solution properties. It is well known that salt is such an external stimulus.<sup>57-59</sup> The effect of NaCl on the rheological properties of the HDPS/SDS hydrogel at  $C_T=50 \text{ mmol}\cdot\text{L}^{-1}$  and  $X_{\text{SDS}}=0.4$  is studied. As Fig. 7 shows the elastic modulus ( $G'$ ) and viscous modulus ( $G''$ ) increase with NaCl concentration. It is suggested that that the hydrogel strength is

gradually enhanced with the increase of NaCl concentration. Further investigations show that salt can also induce sol to gel phase transition. Fig.8 shows the elastic modulus ( $G'$ ) and viscous modulus ( $G''$ ) as a function of the angular frequency ( $\omega$ ) for HDPS/SDS mixed surfactant solution ( $C_T=15 \text{ mmol}\cdot\text{L}^{-1}$ ,  $X_{\text{SDS}}=0.4$ ) without and with  $100 \text{ mmol}\cdot\text{L}^{-1}$  NaCl. It can be seen that the rheological responses of HDPS/SDS mixed solution ( $C_T=15 \text{ mmol}\cdot\text{L}^{-1}$ ,  $X_{\text{SDS}}=0.4$ ) reflect its viscous nature with  $G''$  being much higher than  $G'$  within all measured frequency. Moreover,  $G'$  is smaller than  $0.0001 \text{ Pa}$ . However, after the addition of  $100 \text{ mmol}\cdot\text{L}^{-1}$  NaCl, the sample is dominated elastic with  $G'$  exceeding  $G''$  over the entire range of frequency and  $G'$  is larger than  $100 \text{ Pa}$ . These results imply that the HDPS/SDS mixed solution at  $C_T=15 \text{ mmol}\cdot\text{L}^{-1}$  and  $X_{\text{SDS}}=0.4$  is in a sol state but transit to gel state by adding NaCl.

For the HDPS/SDS mixed solution, the aggregate surface is negative charge. In the presence of NaCl, the binding  $\text{Na}^+$  can continually reduce the repulsion force between surfactant headgroups and increase the critical packing parameter  $p$  of HDPS/SDS system. As a result, adding salt makes the wormlike micelle lengthened and the solution rheological properties reinforced. Even it may induce a sol-gel phase transition.

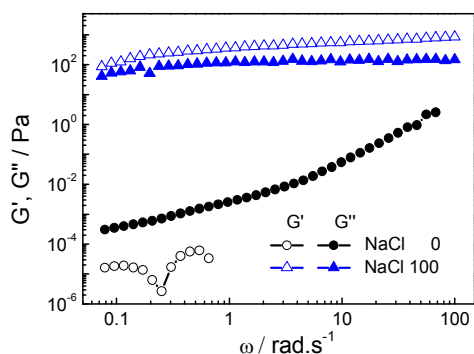


**Fig. 8** Frequency dependence of the elastic modulus ( $G'$ ) and viscous modulus ( $G''$ ) of HDAPS/SDS mixed solution ( $C_T=15 \text{ mmol}\cdot\text{L}^{-1}$ ,  $X_{\text{SDS}}=0.4$ ) without and with  $100 \text{ mmol}\cdot\text{L}^{-1}$  NaCl.

As is mentioned above, only viscoelastic wormlike micelle can be detected in TDPS/SDS mixed surfactant system by adjusting surfactant concentration and molar ratio at the temperature ranging from  $25 \text{ }^\circ\text{C}$  to  $5 \text{ }^\circ\text{C}$ . And it was found that upon adding of NaCl into TDPS/SDS mixed solution, the system has the ability to form gel upon cooling, e.g., the gel-sol transition temperature ( $T_{\text{g-s}}$ ) is about  $17 \text{ }^\circ\text{C}$  for TDPS/SDS system at  $C_T=100 \text{ mmol}\cdot\text{L}^{-1}$  and  $X_{\text{SDS}}=0.4$  in the presence of  $100 \text{ mmol}\cdot\text{L}^{-1}$  NaCl. Fig.9 shows the effect of NaCl on the rheological responses of TDPS/SDS system at  $15 \text{ }^\circ\text{C}$ . The dynamic stress sweep experiment of TDPS/SDS solution ( $C_T=100 \text{ mmol}\cdot\text{L}^{-1}$ ,  $X_{\text{SDS}}=0.4$ ) only shows viscous modulus (Fig.9a). Upon increasing the concentration of NaCl, it also shows elastic modulus and both modulus increase. When NaCl concentration more than  $100 \text{ mmol}\cdot\text{L}^{-1}$ , the elastic modulus ( $G'$ ) exceeds viscous modulus ( $G''$ ) and  $G'$  is larger than  $100 \text{ Pa}$  (Fig.9b). Moreover, the changes of  $G'$  and  $G''$  with frequency is very similar to HDPS/SDS hydrogel for TDPS/SDS solution with  $100 \text{ mmol}\cdot\text{L}^{-1}$  NaCl. All these results also

confirm the phenomenon of salt-induced sol-gel transition for mixed zwitterionic and anionic surfactant systems.

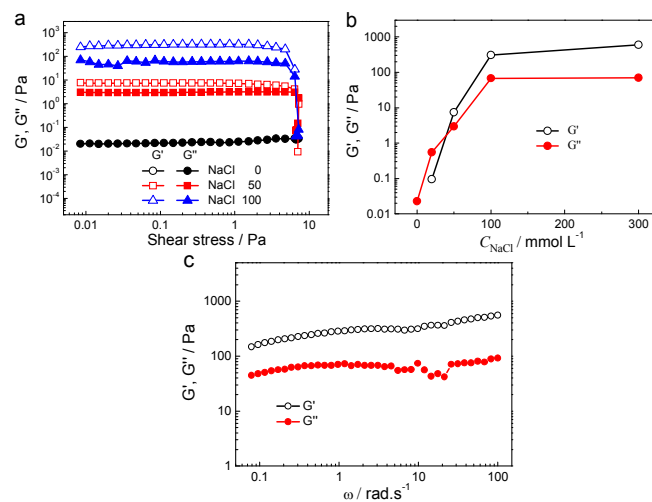


**Fig. 9** At  $15 \text{ }^\circ\text{C}$ , rheological responses of TDPS/SDS mixed solutions ( $C_T=100 \text{ mmol}\cdot\text{L}^{-1}$ ,  $X_{\text{SDS}}=0.4$ ) in the presence of NaCl: (a) dynamic stress sweep at a fixed angular frequency ( $\omega=1 \text{ rad}\cdot\text{s}^{-1}$ ); (b) Elastic modulus ( $G'$ ) and viscous modulus ( $G''$ ) as functions of NaCl concentration; (c) Frequency dependence of the elastic modulus ( $G'$ ) and viscous modulus ( $G''$ ) with  $100 \text{ mmol}\cdot\text{L}^{-1}$  NaCl.

## Conclusions

In the present study, the phase behavior and microstructures are studied in the mixed system of zwitterionic surfactant N-hexadecyl-N,N-dimethyl-3-ammonio-1-propane sulfonate (HDPS,  $C_{16}$ -saturated tailed) and anionic surfactant sodium dodecylsulfate (SDS). Wormlike micelles and small vesicles are demonstrated to coexist in the HDPS/SDS system and wormlike micelles can prolong and entangle each other to form three-dimensional elastic hydrogel. Using a medium length saturated chain zwitterionic surfactant (HDPS) as hydrogelator avoids the insoluble in water and instability by oxidation and hydrolysis of long chain zwitterionic surfactants containing unsaturated carbon-carbon double bond and amido group as noted by previous literatures.<sup>19, 20, 36</sup> Based on the variation of the temperature and adding salt concentration, the wormlike micelle growth can be controlled and further induced the formation or destruction of the hydrogel. Thus the mixed HDPS/SDS surfactant solution can be easily switched between gel and sol by the dual stimuli responses. These results provided templates for the synthesis of controlled nanomaterials and controlled release carriers for drug release and delivery. It is expected that this study may provide further understanding of the general rules for surfactant-based hydrogel formation and advance hydrogel applications in related fields.

## Acknowledgments

This work is supported by Open Fund of State Key Laboratory of Oil and Gas Reservoir Geology and Exploitation (PLN1302), National Basic Research Program of China (973 Program, 2013CB933800), the NSFC program of China (51104169, 21273286, 21273003, 21473005), Fok Ying Tung Education Foundation

(141047) and the Program for Changjiang Scholars and Innovative Research Team in University (IRT1294).

## Notes and references

<sup>a</sup> College of Petroleum Engineering, China University of Petroleum (East China), Qingdao 266580, Shandong Province, P. R. China. E-mail: HaimingFan@126.com; Fax: +86-532-86981701; Tel: +86-532-86983051

<sup>b</sup> State Key Laboratory of Oil and Gas Reservoir Geology and Exploitation, Southwest Petroleum University, Chengdu 610500, Sichuan Province, P. R. China.

<sup>c</sup> Beijing National Laboratory for Molecular Sciences (BNLMS), State Key Laboratory for Structural Chemistry of Unstable and Stable Species, College of Chemistry, Peking University, Beijing 100871, P. R. China. E-mail: JBHuang@pku.edu.cn; Fax: +86-10-62751708; Tel: +86-10-62753557

- 1 H. J. van der Linden, S. Herber, W. Olthuisa and P. Bergveld, *Analyst*, 2003, **128**, 325-331.
- 2 Z.Q. Tou, T.W. Koh and C.C. Chan, *Sensors and Actuators B: Chemical*, 2014, **202**, 185–193.
- 3 A. L. Butcher, G. S. Offeddu and M. L. Oyen, *Trends in Biotechnology*, 2014, **32**, 564–570.
- 4 C. C. Huang, S. Ravindran, Z. Y. Yin and A. George, *Biomaterials*, 2014, **35**, 5316–5326.
- 5 A. Döring, W. Birnbauma and D. Kuckling, *Chem. Soc. Rev.*, 2013, **42**, 7391-7420.
- 6 D. Das, T. Kara and P. K. Das, *Soft Matter*, 2012, **8**, 2348-2365.
- 7 Y. Qiao, Y. Y. Lin, S. F. Zhang and J. B. Huang, *Chem. Eur. J.*, 2011, **17**, 5180–5187.
- 8 Y. Y. Lin, Y. Qiao, C. Gao, P. F. Tang, Y. Liu, Z. B. Li, Y. Yan and J. B. Huang, *Chem. Mater.*, 2010, **22**, 6711–6717.
- 9 J. C. Tiller, *Angew. Chem. Int. Ed.*, 2003, **42**, 3072-3075.
- 10 A.R. Fajardo, M. B. Silva, L.C. Lopes, J. F. Piai, A.F. Rubira and E. C. Muniz, *RSC Adv.*, 2002, **2**, 11095-11103.
- 11 Y. Osada and A. R. Khokhlov (Eds.), *Polymer Gels and Networks*, Marcel Dekker, New York, USA, 2002.
- 12 Y.G. Kim, C. H. Lee and Y. C. Bae, *Fluid Phase Equilibria*, 2014, **361**, 200–207.
- 13 P. Terech and R. G. Wiess (Eds.), *Molecular Gels*, Kluwer Academic Publishers, The Netherlands, 2004.
- 14 L. A. Estroff and A. D. Hamilton, *Chem. Rev.*, 2004, **104**, 1201-1217.
- 15 M. Kodama and S. Sekib, *Adv. Colloid Interface Sci.*, 1991, **35**, 1–30.
- 16 H. Hoffmann and W. Ulbricht, *Curr. Opin. Colloid. Interface. Sci.*, 1996, **1**, 726-739.
- 17 K. Trickett and J. Eastoe, *Adv. Colloid Interface Sci.*, 2008, **144**, 66–74.
- 18 S. R. Raghavan and J. F. Douglas, *Soft Matter*, 2012, **8**, 8539-8546.
- 19 R. Kumar, G. C. Kalur, L. Ziserman, D. Danino and S. R. Raghavan, *Langmuir*, 2007, **23**, 12849–12856.
- 20 Z. L. Chu and Y. J. Feng, *Chem. Commun.*, 2011, **47**, 7191-7193.
- 21 L. Zhao, K. Wang, L. M. Xu, Y. Liu, S. Zhang, Z. B. Li, Y. Yan and J. B. Huang, *Soft Matter*, 2012, **8**, 9079–9085.
- 22 Y.Y.Lin, X.Han, J.B.Huang, H. L. Fu and C.L. Yu, *J. Colloid and Interface Sci.*, 2009, **330**, 449–455.
- 23 H.S. Lu, L. Wang and Z.Y. Huang, *RSC Adv.*, 2014, **4**, 51519-51527.
- 24 H. Hoffmann, C. Thunig, P. Schmiedel and U. Munkert, *Faraday Discuss.*, 1995, **101**, 319-333.
- 25 M. Gradzielski, M. Bergmeier, H. Hoffmann, M. Müller and I. Grillo, *J. Phys. Chem. B*, 2000, **104**, 11594-11597.
- 26 M. Yang, J.C. Hao and H. G. Li, *RSC Adv.*, 2014, **4**, 40595-40605.
- 27 N. Duerr-Auster, J. Kohlbrecher, T. Zuercher, R. Gunde, P. Fischer and E. Windhab, *Langmuir*, 2007, **23**, 12827–12834.
- 28 Y. Kawabata, A. Matsuno, T. Shinoda and T. Kato, *J. Phys. Chem. B*, 2009, **113**, 5686–5689.
- 29 P.F. Long and J. C. Hao, *Soft Matter*, 2010, **6**, 4350-4356.
- 30 I. Nakazawa, M. Masuda, Y. Okada, T. Hanada, K. Yase, M. Asai and T. Shimizu, *Langmuir*, 1999, **15**, 4757–4764.
- 31 T. Imae, N. Hayashi, T. Matsumoto, T. Tada and M. Furusaka, *J. Colloid Interface Sci.*, 2000, **225**, 285–290.
- 32 D. Berthier, T. Buffeteau, J. M. Leger, R. Oda and I. Huc, *J. Am. Chem. Soc.*, 2002, **124**, 13486-13494.
- 33 Y. T. Wang, X. Xin, W.Z. Li, C. Y. Jia, L. Wang, J. L. Shen and G. Y. Xu, *J. Colloid and Interface Sci.*, 2014, **431**, 82–89.
- 34 Y. I. González and E.W. Kaler, *Langmuir*, 2005, **21**, 7191–7199.
- 35 Y.Y. Lin, Y. Qiao, Y. Yan and J. B. Huang, *Soft Matter*, 2009, **5**, 3047–3053.
- 36 Z. L. Chu, Y. J. Feng, H. Q. Sun, Z.Q. Li, X.W. Song, Y.G. Han and H.Y. Wang, *Soft Matter*, 2011, **7**, 4485-4489.
- 37 L. X. Jiang, Y. Yan and J. B. Huang, *Soft Matter*, 2011, **7**, 10417-10423.
- 38 K. Golemanov, N. D. Denkov, S. Tcholakova, M. Vethamuthu and A. Lips, *Langmuir*, 2008, **24**, 9956-9961.
- 39 D. Lopez-Diaz, E. Sarmiento-Gomez, C. Garza and R. Castillo, *J. Colloid and Interface Sci.*, 2010, **348**, 152–158.
- 40 Y. Qiao, Y. Y. Lin, Y.J. Wang, Z. B. Li and J. B. Huang, *Langmuir*, 2011, **27**, 1718–1723.
- 41 H. M. Fan, X. Y. Wu, S. R. Liu, Y. J. Wang, Y. Li and W. L. Kang, *Acta Chim. Sinica*, 2011, **69**, 1997-2002.
- 42 S.K. Mehta, Khushwinder Kaur, Rishu and K.K. Bhasin, *J. Colloid and Interface Sci.*, 2009, **336**, 322–328.
- 43 L. Brinchi, R. Germani, P. Di Profio, L. Marte, G. Savelli, R. Oda and D. Berti, *J. Colloid and Interface Sci.*, 2010, **346**, 100–106.
- 44 X. Z. Wang, W. L. Kang, X. C. Meng, H.M. Fan, H. Xu, J. B. Fu and Y. N. Zhang, *Acta Phys. -Chim. Sin.*, 2012, **28**, 2285-2290.
- 45 J. H. Zhao, C. L. Dai, Q. F. Ding, M. Y. Du, H. S. Feng, Z. Y. Wei, A. Chen and M. W. Zhao, *RSC Adv.*, DOI: 10.1039/C4RA16235H.
- 46 M. Tiecco, G. Cardinali, L. Roscini, R. Germani and L. Corte, *Colloids Surf. B: Biointerfaces* 2013, **111**, 407–417.
- 47 D. Saul, G. J. T. Tiddy, B. A. Wheeler, P. A. Wheeler, E. Willis, *J. Chem. Soc., Faraday Trans. 1* 1974, **70**, 163–170.
- 48 O. Mengual, G. Meunier, I. Cayré, K. Puech and P. Snabre, *Talanta*, 1999, **50**, 445–456.
- 49 Y. Yan, H. Hoffmann, Y. Talmon, A. Makarsky and W. Richter, *J. Phys. Chem. B*, 2007, **111**, 6374-6382.
- 50 Y. W. Shen, H. Hoffmann and J. C. Hao, *Langmuir*, 2009, **25**, 10540-10547.
- 51 H. M. Fan, B. C. Li, Y. Yan, J. B. Huang and W. L. Kang, *Soft matter*, 2014, **10**, 4506-4512.
- 52 R.G. Larson, *The Structure and Rheology of Complex Fluids*, Oxford University Press, New York, USA, 1999.

## Journal Name

- 53 J. N. Israelachvili, D. J. Mitchell and B. W. Ninham, *J. Chem. Soc. Faraday Trans.*, 1976, **272**, 1525-1567.
- 54 R. A. Khalil and A. A. Zarari, *Applied Surface Science*, 2014, **318**, 85–89.
- 55 L. Li, H. Shan, Y. Yue, Y.C. Lam, K.C. Tam and X. Hu, *Langmuir*, 2002, **18**, 7291-7298.
- 56 M. Tomšič, F. Prossnigg and O. Glatter, *J. Colloid and Interface Sci.*, 2008, **322**, 41–50.
- 57 P. A. Hassan, S. R. Raghavan and E. W. Kaler, *Langmuir*, 2002, **18**, 2543-2548.
- 58 H. M. Fan, Y. Yan, Z. C. Li, Y. Xu, L. X. Jiang, L. M. Xu, B. Zhang and J. B. Huang, *J. Colloid and Interface Sci.*, 2010, **348**, 491-497.
- 59 P. Koshy, V. K. Aswal, M. Venkatesh and P. A. Hassan, *Soft Matter*, 2011, **7**, 4778-4786.